Evidence of two plastic regimes controlled by dislocation nucleation in silicon nanostructures

Julien Godet,[a] Pierre Hirel, Sandrine Brochard, and Laurent Pizzagalli
PhyMat, UMR 6630, Université de Poitiers, CNRS, SP2MI, BP 30179, 86962 Chasseneuil-Futuroscope Cedex, France

(Received 10 October 2008; accepted 12 December 2008; published online 28 January 2009)

We performed molecular dynamics simulations of silicon nanostructures submitted to various stresses and temperatures. For a given stress orientation, a transition in the onset of silicon plasticity is revealed depending on the temperature and stress magnitude. At high temperature and low stress, partial dislocation loops are nucleated in the {111} glide set planes. But at low temperature and very high stress, perfect dislocation loops are formed in the other set of {111} planes called shuffle. This result confirmed by three different classical potentials suggests that plasticity in silicon nanostructures could be controlled by dislocation nucleation. © *2009 American Institute of Physics*.
[DOI: 10.1063/1.3072707]

The silicon nanostructures are currently attracting considerable interest for the nanotechnology since their sizes and electronic properties are tunable.[1,2] For example, Si nanowires are being considered in the development of the future generation of Si-based field effect transistor.[3] In such system the Si crystalline structures can be strained up to 12%,[4] much higher than in bulk silicon. At such level of stress, dislocations may appear,[5] which can strongly degrade the electronic properties of the microelectronic devices.[6] A better understanding of the plastic behavior of silicon nanostructure is then required to continue the silicon-based nanotechnology development.

One major difference between bulk and nanostructures for plasticity partially lies in the process of dislocation formation.[7] In bulk, dislocations are multiplied by mechanisms such as Frank-Read,[8] but in nanostructures such as nanowires or in thin layers, the small dimensions prevent those mechanisms and dislocations are preferentially nucleated from surface irregularities.[9–15] An additional complexity comes from the silicon cubic diamond structure, which is composed of two sets of {111} slip planes: the shuffle and the glide (Fig. 1).[17] Both sets appear active in the bulk plasticity depending on the experimental conditions. At high temperature and low stress, partial dislocations are located in the glide set plane,[18] while at low temperature and high confining pressure only perfect dislocations are mobile and probably located in the shuffle set plane.[19] The presence of two slip planes in the cubic diamond structure has also been used to explain the brittle-ductile transition of silicon.[20] The importance of both sets of slip planes in the context of nanostructure plasticity was still not elucidated and is discussed here.

Recently, high precision tensile tests on a silicon nanowire contacted between two atomic force microscopy (AFM) tips[21] showed plastic deformation occurring at very high stress. Unfortunately, such experiments do not provide information on the onset of the plastic deformations. An alternative solution is molecular dynamics simulations, which could give access to the atomistic mechanisms leading to dislocation nucleation. Numerical simulation of Si nanowire tensile tests, based on classical potentials, brought explanations about the nanowire fracture and plasticity.[22] However, they did not consider surface irregularities, which are known to play an important role on plasticity.[9–15] More recently Izumi and Yip[23] investigated the nucleation of a dislocation loop from a sharp corner on silicon. They determined the activation energy and the saddle point configuration at low temperature; however, they did not investigate the onset of plasticity when temperature increases. The comparison of plasticity in silicon nanostructures, which occurs from surfaces and in silicon bulk, is still missing.

In this work we focused on one of the main mechanisms operating in nanostructure plasticity: The dislocation nucleation from surface irregularities submitted to stresses and temperatures. We compared the dislocations formed from the surface to those governing the plasticity in bulk silicon. Through numerous molecular dynamics simulations performed on a large range of stresses and temperatures, we found two fundamentally different plastic behaviors: one at high temperature and low stress where Shockley partial dislocations are nucleated from the surface and propagate in a

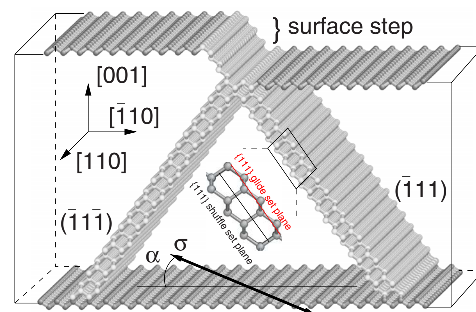

FIG. 1. (Color online) Atomic system modeling a ledge on the (001) silicon surface. Only atoms on the surfaces (dark gray) and inside both slip planes ($\bar{1}1\bar{1}$) and ($\bar{1}11$) (light gray) are represented (Ref. 16). The uniaxial stress σ inside the (001) plane forms an angle α with respect to the [$\bar{1}10$] direction.

[a]Electronic mail: julien.godet@univ-poitiers.fr.

 © 2009 American Institute of Physics

Downloaded 05 Feb 2009 to 194.167.47.253. Redistribution subject to AIP license or copyright; see http://jap.aip.org/jap/copyright.jsp

{111} glide set plane, and the second at low temperature and high stress where perfect dislocations are also emitted from the surface and slip in a {111} shuffle set plane. These results underline two points: Nanostructure plasticity can be controlled by dislocation nucleations from surfaces, and then this process is only governed by the temperature and the stress magnitude.

To model the surface of a silicon nanostructure, we generated the parallelepiped structure represented in Fig. 1. The surface irregularity is composed of several atomic layers, up to five, forming a ledge with a {111} face. Both bottom and upper surfaces are free and $p(2\times1)$ reconstructed.[24] Periodic boundary conditions have been used along the step line, and we kept frozen both $\{\bar{1}10\}$ surfaces in the last direction for maintaining the applied stress. The atomic system contains around 40 000 atoms distributed in 36 atomic layers along the step line, but bigger systems up to 150 000 atoms are also tested without significant differences. We considered three interatomic potentials to describe the Si–Si interaction: Stillinger–Weber (SW),[25] Tersoff,[26] and the environment dependent interatomic potential (EDIP).[27] To simulate the effect of the applied uniaxial stress σ (Fig. 1), the system has been deformed according to the strains calculated using the silicon compliances S_{ijkl}.[17] We obtained the S_{ijkl} from the elastic constants C_{ijkl}, computed for all empirical potentials. The uniaxial stress is contained into the (001) plane, and its direction can be disorientated with an angle α with respect to the $[\bar{1}10]$ direction (Fig. 1). Molecular dynamics simulation have been performed on a time scale ranging from 50 to 400 ps, with a time step of 0.5 fs and for temperatures ranging from 0 to 1500 K.

To investigate the different plastic mode of our systems under tensile stresses, we chose the molecular dynamics simulation performed for a stress orientation $\alpha=18°$. This leads to a resolved shear stress inside the {111} slip planes approximately equivalent for three different dislocations:[28] the 90° head partial, the 30° queue partial, and the 60° perfect. For clarity, we only present the results obtained by the classical potential of SW. The differences obtained with other potentials will be discussed later.

For the low temperature and large stress domain, we considered as an example a simulation performed at 600 K and for a strain about 13.2%. We note that very large stresses are relatively common in perfect nanostructures;[4,7,14,21] however, they are still lower than the theoretical yield stress of Si.[28] After a few picoseconds, the tensile stress is relaxed by the nucleation of a perfect dislocation loop in the {111} shuffle set plane (Fig. 1) increasing the step height [Fig. 2(a)]. A similar dislocation has already been nucleated from a sharp corner during a molecular dynamics simulation performed at 1 K by Izumi *et al.*[23] A short damping of the atomic structure has been done to remove the thermal agitation and to keep the dislocation on site. The dislocation is characterized by a Burgers vector $\vec{b}=1/2[01\bar{1}]$ and forms a half loop connected to the (001) free surface in points A and E. The half loop is composed by two 60° dislocation segments AB and BC and two screw segments CD and DE separated by a kink[29] in D [Fig. 2(a)]. The core structure of

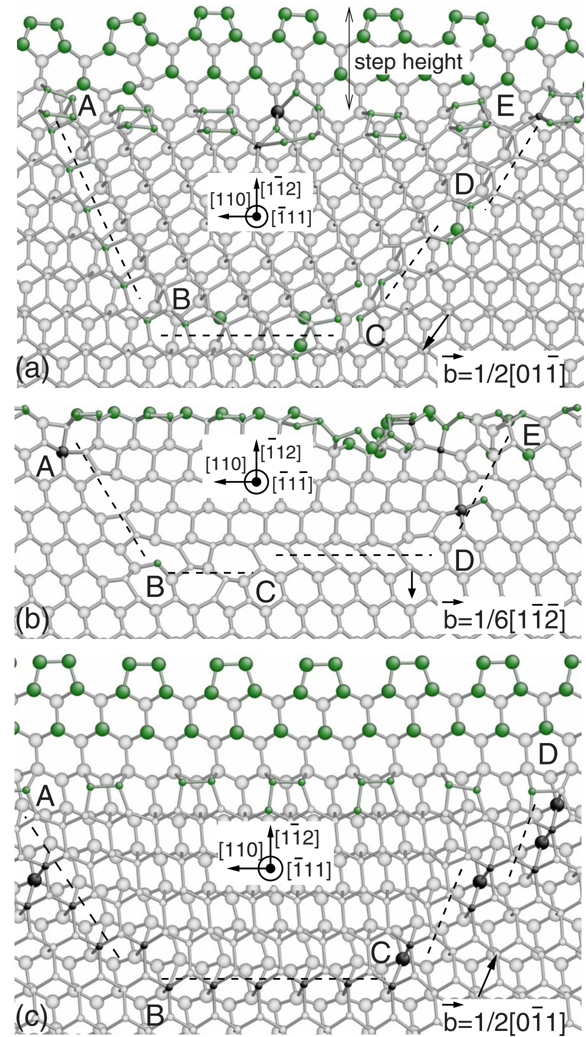

FIG. 2. (Color online) Atomic configurations of dislocations nucleated in different {111} slip planes. The dashed line is a guide to the eyes emphasizing the dislocation position. The Si atoms located below (above) the slip plane are represented by large (small) balls. The dark gray (green), light gray, and black balls correspond to three-, four-, and fivefold coordinated Si atoms, respectively (Ref. 16). Bonds are drawn on distance criteria. [(a) and (c)] Perfect dislocations nucleated in the $(\bar{1}11)$ shuffle set plane at low temperature and large (a) tensile stress or (c) compressive stress. (b) Partial dislocation nucleated in the $(\bar{1}1\bar{1})$ glide set plane at high temperature and low tensile stress.

the perfect 60° dislocation includes threefold coordinated atoms as already observed in *ab initio* calculations.[14] The screw segment is mainly found in one of its stable configurations given by the SW potential.[30,31] We recall that Fig. 2 is a snapshot of molecular dynamics simulation, which depicts the dislocation configuration during its propagation in temperature, and does not correspond to the equilibrium position of the dislocation.

For the high temperature and low stress domain, we now considered the same system but submitted to a lower strain of about 8.4% and a higher temperature of 1350 K. After 200 ps a partial dislocation embryo, characterized by a Burgers vector $\vec{b}=1/6[1\bar{1}\bar{2}]$, appears in the second set of {111} slip planes called glide (Fig. 1). This dislocation propagates by the formation and migration of double kinks and tends to be aligned along the ⟨110⟩ Peierls valleys of silicon [Fig. 2(b)].

Downloaded 05 Feb 2009 to 194.167.47.253. Redistribution subject to AIP license or copyright; see http://jap.aip.org/jap/copyright.jsp

The half loop emerges at the surface step in points A and E and is composed by two 30° dislocation segments AB and DE, and one 90° dislocation segment BD [Fig. 2(b)]. We easily identify the double period reconstruction of the 30° dislocation on the AB part, as already calculated by classical potentials[32] and tight binding methods.[33] The 90° dislocation is slightly more complex with a double period reconstruction[34] on BC and an asymmetric simple period reconstruction[35] on CD connected by a partial kink[36] in C. We note that the asymmetric simple period reconstruction usually unstable with the SW potential is made possible by the disorientated applied stress.

Under tensile stress, our simulations show dislocation nucleations from surfaces according to two plastic regimes: one at high temperature and low stress where dislocations appear in the {111} glide set planes, and one at low temperature and very large stress where they occur in the {111} shuffle set planes. To confirm this result we performed simulations on the same system but under compressive stress. We chose a stress orientation $\alpha=45°$ favoring three dislocations: the perfects 60° and screw, and the partial 30°.[28] At high temperature (1200 K) and low stress (−6.3%), we observed a spurious linear defect[37] due to the SW potential. However, at low temperature (600 K) and large stress (−11.2%), the step height decreases and a perfect dislocation loop is nucleated in the {111} shuffle set plane [Fig. 2(c)] in agreement with the results in traction. The nucleated dislocation has a Burgers vector $\vec{b}=1/2[0\bar{1}1]$, and is mainly lying along the ⟨110⟩ Peierls valley of silicon giving rise to two 60° segments AB and BC and one screw segment CD [Fig. 2(c)]. The dislocation core structure is similar to the one in Fig. 2(a), but the core atoms are fivefold coordinated probably due to the compressive stress, which brings the atoms closer. The lower silicon elastic limit in compression than in traction is a known feature of the anharmonic potential well of silicon atoms.

The absence of transferability of the classical potential led us to repeat the simulations with two other potentials Tersoff and EDIP for confirming the plastic transition between the glide and the shuffle set. With both potentials we qualitatively observed the same transition depending on the temperature and the applied stress. However, small differences due to the empirical potential have been noted. The glide regime is only obtained in traction (10.8%, 1500 K) with the Tersoff potential whereas it is only observed in compression with EDIP (−6.3%, 1300 K). In the latter case, the partial dislocation loop emerges from the surface step after a premelting of the surface. It has a Burgers vector $\vec{b}=1/6[\bar{1}\bar{2}1]$ and is composed by two 30° segments and one 90° segment. In the shuffle set, plasticity occurs in compression (−7.4%, 300 K) and in traction (11.5%, 600 K) for EDIP, but only in compression for the Tersoff potential (−12.4%, 900 K). Overall the dislocation core structures are similar to those simulated by the SW potential, except for the screw dislocation core that is mainly found in another known configuration.[30,31] We also note that the spurious behavior of EDIP in compression[28] introduced a large shear stress of the {111} shuffle set plane before the nucleation of the perfect dislocation.

In conclusion, our calculations based on three different classical potentials revealed dislocation nucleation from surface irregularities when they are submitted to stress. According to the temperature and the stress magnitude two distinct regimes of plasticity have been observed: one at high temperature and low stress where dislocations propagate in the glide set planes and one at low temperature and high stress where dislocations propagate in the shuffle set planes. However, compared to the bulk silicon, the only source of dislocations comes from the surface. The dislocation nucleation from the surface then appears as the main mechanism that governs the plasticity in nanostructures.

[1] Y. Cui, L. J. Lauhon, M. S. Gudiksen, J. Wang, and C. M. Lieber, Appl. Phys. Lett. **78**, 2214 (2001).
[2] K. Byon, D. Tham, J. E. Fischer, and A. T. Johnson, Appl. Phys. Lett. **87**, 193104 (2005).
[3] Y. Cui and C. M. Lieber, Science **291**, 851 (2001).
[4] K.-C. Lu, W.-W. Wu, H.-W. Wu, C. M. Tanner, J. P. Chang, L. J. Chen, and K. N. Tu, Nano Lett. **7**, 2389 (2007).
[5] R. X. Wu and G. C. Weatherly, Philos. Mag. A **81**, 1489 (2001).
[6] S. M. Hu, J. Appl. Phys. **70**, R53 (1991).
[7] M. D. Uchic, D. M. Dimiduk, J. N. Florando, and W. D. Nix, Science **305**, 986 (2004).
[8] A. Moulin, M. Condat, and L. P. Kubin, Philos. Mag. A **79**, 1995 (1999).
[9] X. J. Ning and N. Huvey, Philos. Mag. Lett. **74**, 241 (1996).
[10] G. Xu, A. S. Argon, and M. Ortiz, Philos. Mag. A **75**, 341 (1997).
[11] S. Brochard, P. Beauchamp, and J. Grilhé, Philos. Mag. A **80**, 503 (2000).
[12] B. J. Gally and A. S. Argon, Philos. Mag. A **81**, 699 (2001).
[13] A. S. Argon and B. J. Gally, Scr. Mater. **45**, 1287 (2001).
[14] J. Godet, S. Brochard, L. Pizzagalli, P. Beauchamp, and J. M. Soler, Phys. Rev. B **73**, 092105 (2006).
[15] P. Hirel, S. Brochard, L. Pizzagalli, and P. Beauchamp, Scr. Mater. **57**, 1141 (2007).
[16] J. Li, Modell. Simul. Mater. Sci. Eng. **11**, 173 (2003).
[17] J. P. Hirth and J. Lothe, *Theory of Dislocations*, 2nd ed. (Wiley, New York, 1982).
[18] I. L. F. Ray and D. J. H. Cockayne, Philos. Mag. **22**, 853 (1970).
[19] J. Rabier, P. Cordier, T. Tondellier, J. L. Demenet, and H. Garem, J. Phys.: Condens. Matter **12**, 10059 (2000).
[20] M. de Koning, A. Antonelli, M. Z. Bazant, E. Kaxiras, and J. F. Justo, Phys. Rev. B **58**, 12555 (1998).
[21] T. Kizuka, Y. Takatani, K. Asaka, and R. Yoshizaki, Phys. Rev. B **72**, 035333 (2005).
[22] K. Kang and W. Cai, Philos. Mag. **87**, 2169 (2007).
[23] S. Izumi and S. Yip, J. Appl. Phys. **104**, 033513 (2008).
[24] D. J. Chadi, Phys. Rev. Lett. **43**, 43 (1979).
[25] F. H. Stillinger and T. A. Weber, Phys. Rev. B **31**, 5262 (1985).
[26] J. Tersoff, Phys. Rev. B **39**, 5566 (1989).
[27] M. Z. Bazant, E. Kaxiras, and J. F. Justo, Phys. Rev. B **56**, 8542 (1997).
[28] J. Godet, S. Brochard, L. Pizzagalli, and P. Beauchamp, Phys. Rev. B **70**, 054109 (2004).
[29] L. Pizzagalli, A. Pedersen, A. Arnaldsson, H. Jónsson, and P. Beauchamp, Phys. Rev. B **77**, 064106 (2008).
[30] H. Koizumi, Y. Kamimura, and T. Suzuki, Philos. Mag. A **80**, 609 (2000).
[31] L. Pizzagalli, P. Beauchamp, and J. Rabier, Philos. Mag. **83**, 1191 (2003).
[32] M. S. Duesbery, B. Joos, and D. J. Michel, Phys. Rev. B **43**, 5143 (1991).
[33] R. W. Nunes, J. Bennetto, and D. Vanderbilt, Phys. Rev. B **57**, 10388 (1998).
[34] J. Bennetto, R. W. Nunes, and D. Vanderbilt, Phys. Rev. Lett. **79**, 245 (1997).
[35] J. R. K. Bigger, D. A. McInnes, A. P. Sutton, M. C. Payne, I. Stich, R. D. King-Smith, D. M. Bird, and L. J. Clarke, Phys. Rev. Lett. **69**, 2224 (1992).
[36] V. V. Bulatov, J. F. Justo, W. Cai, S. Yip, A. S. Argon, T. Lenosky, M. de Koning, and T. Diaz de la Rubia, Philos. Mag. A **81**, 1257 (2001).
[37] J. Godet, L. Pizzagalli, S. Brochard, and P. Beauchamp, Comput. Mater. Sci. **30**, 16 (2004).

Downloaded 05 Feb 2009 to 194.167.47.253. Redistribution subject to AIP license or copyright; see http://jap.aip.org/jap/copyright.jsp